MATHEMATICS AND COMPUTATIONAL SCIENCES

Vol 6(1), 2025, pp:30-43

DOI:10.30511/mcs.2025.2051683.1299

ISSN:2717-2708

http://mcs.qut.ac.ir/

Qom University of Technology

Numerical solution of the viscœlastic wave equation by Galerkin spectral element method

Jalil Rashidinia [1], **Feze Barzegar** [2]

[1,2]School of Mathematics and Computer Science, Iran University of Science and Technology, Tehran, Iran

Abstract: In this paper, the Galerkin spectral element method (GSEM) is presented for solving the one-dimensional viscœlastic wave equation. The finite difference approximation is applied for temporal direction, and the convergence order of the technique is demonstrated. An a priori error estimate is determined for the total-discrete system. The computational efficiency of the method is confirmed through a numerical example, which shows that the method is effectively applicable.

Keywords: Viscœlastic wave equations; Galerkin spectral element method; Error estimate.
2010 Mathematics Subject Classification: 35L75; 74D05; 65N35; 65N15
Receive: 26 January 2025, **Accepted:** 24 February 2025

1 Introduction

The Galerkin spectral element method (GSEM), initially introduced in [22], has become a highly effective numerical technique for solving partial differential equations (PDEs). The nodal SEM uses Lagrange polynomials with Gauss–Lobatto–Legendre (GLL) for interpolation and GLL quadrature for integration to produce a diagonal mass matrix. It facilitates efficient implementation on parallel computers [9, 11, 12]. This method has been successfully applied to various equations, including the acoustic equation [1, 20, 24, 28], Maxwell equation [2], the Pennes bioheat transfer equation [4], Sobolev equation [5], the nonlinear generalized Benjamin–Bona–Mahony–Burgers equation [6], Helmholtz's equation [17], and the p–Laplacian equation [25].
This paper deals with the numerical approximation of the following one–dimensional viscœlastic wave problem:

$$\frac{\partial^2 u(x,t)}{\partial t^2} - \beta \frac{\partial^3 u(x,t)}{\partial t \partial x^2} - \gamma \frac{\partial^2 u(x,t)}{\partial x^2} = f(x,t); \quad (x,t) \in I \times (0,T]. \tag{1.1}$$

Subject to Dirichlet boundary conditions

$$u(X_L,t) = f_L, \quad u(X_R,t) = f_R, \quad t \in [0,T], \tag{1.2}$$

and initial conditions

$$\begin{aligned} u(x,0) &= u_0(x), \quad x \in I, \\ \frac{\partial u(x,0)}{\partial t} &= u_1(x), \qquad x \in I, \end{aligned} \tag{1.3}$$

[1]Corresponding author: rashidinia@iust.ac.ir
[2]Fz.Barzegar92@gmail.com

where $I = [X_L, X_R]$ is a bounded domain in $\mathbb{R}$. β and γ are positive constants and $T > 0$ is the final time. The boundary conditions f_L and f_R are known constants. The source term $f(x,t)$ and initial conditions $u_0(x)$, $u_1(x)$ are known functions with sufficient smoothness.

So far, only a limited number of numerical methods have been proposed for solving the time-dependent viscœlastic equation. Zhao, Li, and Luo [29] applied a space-time continuous Galerkin method with mesh modification, while Li, Zhao, and Luo [15] introduced a space-time continuous finite element method. Xia and Luo [26] presented a classical finite element method and also investigated a finite difference iterative scheme based on the proper orthogonal decomposition (POD) technique in [27, 26]. Luo and Teng [16] developed an optimized splitting positive definite mixed finite element extrapolation approach using the POD technique. Jin and Luo [10] established the Crank–Nicolson (CN) collocation spectral method. Oruc [21] discussed two meshless methods with time marching performed using a fourth-order Runge–Kutta method. Nikan and Avazzadeh [18] combined the CN scheme with the localized meshless technique.

The main result of this paper is the derivation of an a priori error bound for the numerical approximation of the one-dimensional viscœlastic equation using the Gauss–Lobatto–Legendre Galerkin Spectral Element Method (GLL–GSEM). We obtain the rates of convergence in h and p, which align with those observed numerically. The viscœlastic wave equation involves not only second-order derivative terms with respect to time and spatial variables but also a mixed derivative term that includes the first-order derivative with respect to time and the second-order derivative with respect to spatial variables. This additional complexity presents significant challenges for analysis. In the temporal direction, we use the finite difference method with the Crank–Nicolson (CN) approach. This method has been effectively and widely used approach in the meshless, finite element, radial basis function (RBF), and spectral methods nowadays [19, 14, 10].

The structure of this study is as follows: Section 2 covers the variational form of the problem, the time semi-discrete approach, and the order of convergence have been analyzes. In Section 3, the Gauss–Lobatto–Legendre Galerkin Spectral Element Method (GLL–GSEM) is applied for discrete spatial directions and provided an a priori error estimate of the fully-discrete formulation. Finally, Section 4 provides a test problem to validate the accuracy and implementation of our approach.

2 Temporal discretization of the viscœlastic wave equation

To perform the time discretization of the viscœlastic equation, by employing the CN algorithm, we begin by splitting the time interval $[0,T]$ into N_T equal subintervals, each with a size of $k = T/N_T$. The time steps are then defined as $t_n = kn$ for $n = 1, \ldots, N_T$. We use the finite difference discretization in temporal direction

$$\frac{\partial^2 u(x,t)}{\partial t^2} = \frac{1}{k^2}\left[u^{n+1} - 2u^n + u^{n-1}\right] - \frac{k^2}{12}\frac{d^4 u(x,\xi_1)}{dt^4}, \xi_1 \in (t_{n-1}, t_{n+1}), \tag{2.1}$$

$$\frac{\partial^3 u(x,t)}{\partial t \partial x^2} = \frac{1}{2k}\left[\frac{d^2 u^{n+1}}{dx^2} - \frac{d^2 u^{n-1}}{dx^2}\right] - \frac{k^2}{6}\frac{\partial^5 u(x,\xi_2)}{\partial t^3 \partial x^2}, \xi_2 \in (t_{n-1}, t_{n+1}), \tag{2.2}$$

$$\frac{d^2 u(x,t)}{dx^2} = \frac{1}{3}\left[\frac{d^2 u^{n+1}}{dx^2} + \frac{d^2 u^n}{dx^2} + \frac{d^2 u^{n-1}}{dx^2}\right] - \frac{k^2}{3}\frac{\partial^4 u(x,\xi_3)}{\partial t^2 \partial x^2}, \xi_3 \in (t_{n-1}, t_{n+1}). \tag{2.3}$$

By denoting $u^{n+1} = u(x, t_{n+1})$ and $f^{n+1} = f(x, t_{n+1})$ the semi-discrete CN viscœlastic wave equation is:

$$\begin{aligned}\frac{1}{k^2}\left[u^{n+1} - 2u^n + u^{n-1}\right] - \frac{1}{2k}\left[\frac{d^2 u^{n+1}}{dx^2} - \frac{d^2 u^{n-1}}{dx^2}\right] \\ - \frac{1}{3}\left[\frac{d^2 u^{n+1}}{dx^2} + \frac{d^2 u^n}{dx^2} + \frac{d^2 u^{n-1}}{dx^2}\right] = f^{n+1} + k^2 \mathcal{R}_t.\end{aligned} \tag{2.4}$$

where $\mathcal{R}_t$ is the residual with respect to time. For the first iterative, we need the value of u^{-1}, by using the relation

$$\frac{\partial u(x,t)}{\partial t} \xrightarrow{t=0} u_1 \simeq \frac{u^1 - u^{-1}}{2k}, \tag{2.5}$$

we can rewrite the Eq. (2.5) as follows:

$$u^{-1} = u^1 - 2ku_1, \tag{2.6}$$

substituting (2.6) into (2.4), we obtain the scheme for $n = 0$

$$\begin{aligned} 2u^1 - \frac{2\beta k^2}{3}\left(\frac{d^2u^1}{dx^2}\right) =& 2u_0 + 2ku_1 + \frac{\beta k^2}{3}\left(\frac{d^2u_0}{dx^2}\right) + \gamma k^2 u_1 - \frac{2k^3\beta}{3}\left(\frac{d^2u_1}{dx^2}\right) \\ &+ k^2 f^1 + k^2\mathcal{R}_t. \end{aligned} \tag{2.7}$$

By removing the residual $\mathcal{R}_t$, from (2.4) and (2.7), the approximate solution for the semi-discrete CN is obtained. Denoting the approximate solution of u^n by U^n for $n = 1, ..., N_T$, we have

$$\begin{aligned} &\frac{1}{k^2}\left[U^{n+1} - 2U^n + U^{n-1}\right] - \frac{1}{2k}\left[\frac{d^2U^{n+1}}{dx^2} - \frac{d^2U^{n-1}}{dx^2}\right] \\ &- \frac{1}{3}\left[\frac{d^2U^{n+1}}{dx^2} + \frac{d^2U^n}{dx^2} + \frac{d^2U^{n-1}}{dx^2}\right] = f^{n+1}. \end{aligned} \tag{2.8}$$

and for $n = 0$

$$\begin{aligned} 2U^1 - \frac{2\beta k^2}{3}\left(\frac{d^2U^1}{dx^2}\right) &= 2u_0 + 2ku_1 + \frac{\beta k^2}{3}\left(\frac{d^2u_0}{dx^2}\right) \\ &+ \gamma k^2 u_1 - \frac{2k^3\beta}{3}\left(\frac{d^2u_1}{dx^2}\right) + k^2 f^1. \end{aligned} \tag{2.9}$$

where $e^0 = u^0 - U^0 = 0$.

2.1 Convergence of the temporal-discrete formulation

Subsequently, the convergence analysis for the time-discrete problem is presented. For this purpose, we introduce the functional spaces and norms used in this paper that can be found in [13, 8].

Let us introduce the space $L_2(I)$ equipped with the inner product and the corresponding norm

$$(u, z) = \int_{X_L}^{X_R} u(x)z(x)dx, \qquad \|u\| = \sqrt{(u, u)},$$

and the Hilbert space

$$H^s(I) = \{u \in L_2(I); \frac{\partial^\alpha u}{\partial x^\alpha} \in L_2(I), \quad \alpha \in \mathbb{N}, \quad \alpha \leq s\},$$

equipped with the norm and semi-norm

$$\|u\|_s = \left(\sum_{\alpha \leq s} \left\|\frac{\partial^\alpha u}{\partial x^\alpha}\right\|^2\right)^{1/2}, \quad |u|_s = \left(\sum_{\alpha = s} \left\|\frac{\partial^\alpha u}{\partial x^\alpha}\right\|^2\right)^{1/2}$$

We define the subspace V of $H^1(I)$

$$V = H_0^1(I) = \{u \in H^1(I); \quad u(X_L) = u(X_R) = 0\}.$$

It is very important to introduce Poincaré inequality in one dimension as follows:

$$\|u\| \leq C_{\mathcal{P}}|u|_1, \quad \forall u \in V = H_0^1(I). \tag{2.10}$$

We see that

$$\left(\frac{du}{dx}, \frac{du}{dx}\right) = \left\|\frac{du}{dx}\right\| = |u|_1.$$

Without losing generality, we conduct an error assessment of the semi-discrete difference scheme for the values $\beta = \gamma = 1$. In the rest of the paper, we will consider C as a generic positive constant.

Theorem 2.1. *Assume that u^n and U^n are the analytical and approximate solutions of* (2.4) *and* (2.8)*, respectively. Then, the convergence order in time is $\mathcal{O}\left(k^2\right)$.*

Proof. First, by multiplying (2.4) by z and integrating over the domain I, we obtain the corresponding weak formulation as:

$$\begin{aligned}
&\left(u^{n+1}, z\right) - \frac{k}{2}\left(\frac{d^2u^{n+1}}{dx^2}, z\right) - \frac{k^2}{3}\left(\frac{d^2u^{n+1}}{dx^2}, z\right) \\
&= 2\left(u^n, z\right) - \left(u^{n-1}, z\right) - \frac{k}{2}\left(\frac{d^2u^{n-1}}{dx^2}, z\right) + \frac{k^2}{3}\left(\frac{d^2u^n}{dx^2}, z\right) \\
&\quad + \frac{k^2}{3}\left(\frac{d^2u^{n-1}}{dx^2}, z\right) + k^2\left(f^{n+1}, z\right) + k^2\left(\mathcal{R}_t, z\right),
\end{aligned} \tag{2.11}$$

and similarly for (2.8) we have

$$\begin{aligned}
&\left(U^{n+1}, z\right) - \frac{k}{2}\left(\frac{d^2U^{n+1}}{dx^2}, z\right) - \frac{k^2}{3}\left(\frac{d^2U^{n+1}}{dx^2}, z\right) \\
&= 2\left(U^n, z\right) - \left(U^{n-1}, z\right) - \frac{k}{2}\left(\frac{d^2U^{n-1}}{dx^2}, z\right) + \frac{k^2}{3}\left(\frac{d^2U^n}{dx^2}, z\right) \\
&\quad + \frac{k^2}{3}\left(\frac{d^2U^{n-1}}{dx^2}, z\right) + k^2\left(f^{n+1}, z\right).
\end{aligned} \tag{2.12}$$

Subtract (2.12) from (2.11) to arive at

$$\begin{aligned}
&\left(e^{n+1}, z\right) - \frac{k}{2}\left(\frac{d^2e^{n+1}}{dx^2}, z\right) - \frac{k^2}{3}\left(\frac{d^2e^{n+1}}{dx^2}, z\right) \\
&= 2\left(e^n, z\right) - \left(e^{n-1}, z\right) - \frac{k}{2}\left(\frac{d^2e^{n-1}}{dx^2}, z\right) + \frac{k^2}{3}\left(\frac{d^2e^n}{dx^2}, z\right) \\
&\quad + \frac{k^2}{3}\left(\frac{d^2e^{n-1}}{dx^2}, z\right) + k^2\left(\mathcal{R}_t, z\right),
\end{aligned} \tag{2.13}$$

where $e^n = u^n - U^n$.
By taking $z = e^{n+1}$ in (2.13) and applying integration by parts, we derive the following relation

$$\begin{aligned}
&\left(e^{n+1}, e^{n+1}\right) + \frac{k}{2}\left(\frac{de^{n+1}}{dx}, \frac{de^{n+1}}{dx}\right) + \frac{k^2}{3}\left(\frac{de^{n+1}}{dx}, \frac{de^{n+1}}{dx}\right) \\
&\quad = 2\left(e^n, e^{n+1}\right) - \left(e^{n-1}, e^{n+1}\right) + \frac{k}{2}\left(\frac{de^{n-1}}{dx}, \frac{de^{n+1}}{dx}\right) \\
&\quad\quad - \frac{k^2}{3}\left(\frac{de^n}{dx}, \frac{de^{n+1}}{dx}\right) - \frac{k^2}{3}\left(\frac{de^{n-1}}{dx}, \frac{de^{n+1}}{dx}\right) + k^2\left(\mathcal{R}_t, e^{n+1}\right). \qquad (2.14)
\end{aligned}$$

By using the Young and Cauchy-Schwarz inequalities, we get

$$\begin{aligned}
&\left\|e^{n+1}\right\|^2 + \frac{k}{2}\left\|\frac{de^{n+1}}{dx}\right\|^2 + \frac{k^2}{3}\left\|\frac{de^{n+1}}{dx}\right\|^2 \\
&\quad \le \left\|e^n\right\|^2 + \left\|e^{n+1}\right\|^2 + \left\|e^{n-1}\right\|\left\|e^{n+1}\right\| + \frac{k}{2}\left\|\frac{de^{n-1}}{dx}\right\|\left\|\frac{de^{n+1}}{dx}\right\| \\
&\quad\quad + \frac{k^2}{3}\left\|\frac{de^n}{dx}\right\|\left\|\frac{de^{n+1}}{dx}\right\| + \frac{k^2}{3}\left\|\frac{de^{n-1}}{dx}\right\|\left\|\frac{de^{n+1}}{dx}\right\| + \frac{k^2}{2}\left\|\mathcal{R}_t\right\|^2 + \frac{1}{2}\left\|e^{n+1}\right\|^2. \qquad (2.15)
\end{aligned}$$

Taking $C = \left(k/2 + k^2/3\right)$, adding and subtracting the term $C_{\mathcal{P}}^2\left\|\frac{de^{n+1}}{dx}\right\|^2$ to the left hand side as well as employing the Poincaré inequality, we obtain

$$\begin{aligned}
&C_{\mathcal{P}}^2\left\|\frac{de^{n+1}}{dx}\right\|^2 \\
&\quad \le C_{\mathcal{P}}^2\left\|\frac{de^n}{dx}\right\|^2 + (C_{\mathcal{P}}^2 - C)\left\|\frac{de^{n+1}}{dx}\right\|^2 + C_{\mathcal{P}}^2\left\|\frac{de^{n-1}}{dx}\right\|\left\|\frac{de^{n+1}}{dx}\right\| \\
&\quad\quad + \frac{k}{2}\left\|\frac{de^{n-1}}{dx}\right\|\left\|\frac{de^{n+1}}{dx}\right\| + \frac{k^2}{3}\left\|\frac{de^n}{dx}\right\|\left\|\frac{de^{n+1}}{dx}\right\| + \frac{k^2}{3}\left\|\frac{de^{n-1}}{dx}\right\|\left\|\frac{de^{n+1}}{dx}\right\| \\
&\quad\quad + \frac{C_{\mathcal{P}}^2}{2}\left\|\frac{de^{n+1}}{dx}\right\|\left\|\frac{de^{n+1}}{dx}\right\| + \frac{k^2}{2}\|\mathcal{R}_t\|^2 \qquad (2.16)
\end{aligned}$$

We consider $\left\|\frac{de^J}{dx}\right\| = \max_{0\le j\le N_T}\left\|\frac{de^j}{dx}\right\|$ and take summation terms from 0 to n ($1 \le n \le N_T - 1$), it follows that

$$\begin{aligned}
\left\|\frac{de^{n+1}}{dx}\right\|\left\|\frac{de^J}{dx}\right\| &\le \left\|\frac{de^0}{dx}\right\|\left\|\frac{de^J}{dx}\right\| + C\sum_{j=0}^{n}\left\|\frac{de^J}{dx}\right\|\left\|\frac{de^{j+1}}{dx}\right\| + \sum_{j=0}^{n}\left\|\frac{de^J}{dx}\right\|\left\|\frac{de^{j+1}}{dx}\right\| \\
&\quad + \frac{k}{2C_{\mathcal{P}}^2}\sum_{j=0}^{n}\left\|\frac{de^J}{dx}\right\|\left\|\frac{de^{j+1}}{dx}\right\| + \frac{k^2}{3C_{\mathcal{P}}^2}\sum_{j=0}^{n}\left\|\frac{de^J}{dx}\right\|\left\|\frac{de^{j+1}}{dx}\right\| \\
&\quad + \frac{k^2}{3C_{\mathcal{P}}^2}\sum_{j=0}^{n}\left\|\frac{de^J}{dx}\right\|\left\|\frac{de^{j+1}}{dx}\right\| + \frac{k^2}{2C_{\mathcal{P}}^2}\sum_{j=0}^{n}\|\mathcal{R}_t\|^2. \qquad (2.17)
\end{aligned}$$

By factoring the maximum value, we have

$$\left\|\frac{de^{n+1}}{dx}\right\| \le \left\|\frac{de^0}{dx}\right\| + \frac{k^2}{2C_{\mathcal{P}}^2}\sum_{j=1}^{n}\|\mathcal{R}_t\|^2 + \left(C + 1 + \frac{1}{2C_{\mathcal{P}}^2}k + \frac{2}{3C_{\mathcal{P}}^2}k^2\right)\sum_{j=1}^{n}\left\|\frac{de^{j+1}}{dx}\right\|. \qquad (2.18)$$

Using the discrete Gronwall's inequality

$$\left\|\frac{de^{n+1}}{dx}\right\| \leq \left(\left\|\frac{de^{0}}{dx}\right\| + \frac{k^2}{2C_{\mathcal{P}}^2}\sum_{j=1}^{n}\|\mathcal{R}_t\|^2\right)\exp\left(\sum_{j=1}^{n}\left(C+1+\frac{1}{2C_{\mathcal{P}}^2}k+\frac{2}{3C_{\mathcal{P}}^2}k^2\right)\right). \tag{2.19}$$

Considering $\nabla e^0 = 0$ and $N_T k = T$, and Using the fact that $\|R^t\| \leq k^2$, we conclude that

$$C_{\mathcal{P}}\left\|\frac{de^{n+1}}{dx}\right\| \leq CT^2k^2 exp\left(L+\frac{CT}{C_{\mathcal{P}}^2}+\frac{CT^2}{C_{\mathcal{P}}^2}\right), \tag{2.20}$$

where L is a constant. By employing the Poincaré inequality, we obtain

$$\|e^{n+1}\| \leq C\left(C_{\mathcal{P}}, T\right)k^2, \tag{2.21}$$

which proves the proof. □

3 Galerkin spectral element method and error estimate

This section presents the Galerkin spectral element method (GSEM) using Gauss–Lobatto–Legendre (GLL) nodes. High-order Lagrange interpolation polynomials may lead to Runge's oscillations when approximating the unknown function in each element [7]. However, this phenomenon dœs not occur when using Lagrange interpolation based on GLL nodes [23]. We describe the GLL–GSEM in one dimension.

3.1 Spectral element method in one-dimension

As is typical in grid-based approaches, we begin by dividing the one-dimensional physical domain into N_e non-overlapping elements. We denote the uniform partition of $I = [X_L, X_R]$ by X_h as

$$X_h : X_L = x^{(0)} < x^{(1)} < x^{(2)} < \cdots < x^{(N_e)} = X_R.$$

The l-th element is defined as

$$\mathcal{E}_l = \left\{x | x^{(l-1)} \leq x \leq x^{(l)}\right\}, \quad 1 \leq l \leq N_e,$$

which $I = \cup_{l=1}^{N_e}\mathcal{E}_l$. Each element $\mathcal{E} \in X_h$ can be obtained by a affine map $\mathcal{F}_{\mathcal{E}}$ from a reference element $\hat{\mathcal{E}} = \{\eta | -1 \leq \eta \leq 1\}$ such that $\mathcal{F}_{\mathcal{E}} : \hat{\mathcal{E}} \longrightarrow \mathcal{E}$, $x_{\mathcal{E}} = \mathcal{F}_{\mathcal{E}}(\eta)$, in which

$$x(\eta) = \frac{1}{2}\left[\left(x^{(l)} - x^{(l-1)}\right)\eta + \left(x^{(l)} + x^{(l-1)}\right)\right].$$

The Jacobian of the affine map is

$$\mathrm{J}_l = \frac{\partial x}{\partial \eta} = \frac{x^{(l)} - x^{(l-1)}}{2}.$$

For the unknown function u on the element $\mathcal{E}_l$, the approximation solution of order m is considered as follows

$$u_m^{(\mathcal{E}_l)}(x,t) = \sum_{i=0}^{m} u_m^{(\mathcal{E}_l)}(x_i,t)\,\psi_i(x),$$

in which $\psi_i(x)$ represents the m-degree Lagrange interpolation polynomials, and $\left\{u_m^{(\mathcal{E}_l)}(x_i,t)\right\}_{i=0}^{m}$ indicates the approximate solution at the interpolation points on the element $\mathcal{E}_l$, which correspond to the GLL nodes on the reference element $\hat{\mathcal{E}}$.

The GLL nodes are determined by finding the roots of the equation $Z(\eta) = \left(1-\eta^2\right) \mathrm{Lo}_{m-1}(\eta)$, where Lo_{m-1} is the Lobatto poly. of degree $(m-1)$, derived from the m-degree Legendre poly. $\mathrm{L}_m(\eta)$ as $\mathrm{Lo}_{m-1}(\eta) = \mathrm{L}_m^{'}(\eta)$. The endpoints correspond to $\eta_0 = -1$, $\eta_m = 1$, while the remaining $m-1$ points, $\{\eta_i\}_{i=1}^{m-1}$, are the roots of the derivative of the Legendre polynomials, with all points $\eta_0, \ldots, \eta_m$ lying within the interval $[-1, 1]$.
The m-degree Lagrange polynomials related to the GLL nodes are derived by

$$\psi_i(\eta) = \frac{1}{m(m+1)\,\mathrm{L}_m(\eta_i)} \times \frac{\left(\eta^2-1\right)\mathrm{Lo}_{m-1}(\eta)}{(\eta-\eta_i)}, \quad 0 \le i \le m. \tag{3.1}$$

The element mass matrix related to the element $\mathcal{E}_l$, is obtained

$$A_{i,j}^{(l)} = \int_{x^{(l-1)}}^{x^{(l)}} \psi_i(x)\psi_j(x)dx = \mathrm{J}_l \int_{-1}^{1} \psi_i(\eta)\,\psi_j(\eta)\,d\eta = \mathrm{J}_l \int_{-1}^{1} \Theta_{i,j}(\eta)\,d\eta, \quad 0 \le i,j \le m. \tag{3.2}$$

We defined $\Theta_{i,j}(\eta) = \psi_i(\eta)\,\psi_j(\eta)$ such that

$$A_{i,j}^{(l)} = \mathrm{J}_l \int_{-1}^{1} \Theta_{i,j}(\eta)\,d\eta, \quad 0 \le i,j \le m. \tag{3.3}$$

The integral on the right-hand side of (3.3) is numerically computed. The k-point Lobatto integration quadrature, provides us with the approximation

$$\int_{-1}^{1} \Theta_{i,j}(\eta)\,d\eta = \sum_{s=0}^{k} \Theta_{i,j}(\eta_s)\,W_s, \quad 0 \le i,j \le m,$$

where

$$W_s = \frac{2}{m(m+1)\left[\mathrm{L}_m(\eta_s)\right]^2}, \quad 0 \le s \le k.$$

We note that $\Theta_{i,j}$ is a $2m$-degree poly. in η, the Lobatto quadrature is exact if $k > m$.
The element diffusion matrix related to the element $\mathcal{E}_l$, is given by

$$B_{i,j}^{(l)} = \int_{x^{(l-1)}}^{x^{(l)}} \frac{d\psi_i(x)}{dx}\frac{d\psi_j(x)}{dx}dx = \frac{1}{\mathrm{J}_l}\int_{-1}^{1} \frac{d\psi_i(\eta)}{d\eta}\frac{d\psi_j(\eta)}{d\eta}d\eta, \quad 0 \le i,j \le m, \tag{3.4}$$

We defined $\Psi_{i,j}(\eta) = \dfrac{d\psi_i(\eta)}{dx}\dfrac{d\psi_j(\eta)}{dx}$,

$$B_{i,j}^{(l)} = \frac{1}{\mathrm{J}_l}\int_{-1}^{1} \Psi_{i,j}(\eta)\,d\eta = \frac{1}{\mathrm{J}_l}\sum_{s=0}^{k} \Psi_{i,j}(\eta_s)\,W_s, \quad 0 \le i,j \le m. \tag{3.5}$$

Since $\Psi_{i,j}$ is a $(2m-2)$-degree poly. in η, the Lobatto quadrature is exact if $k = m$. Following [23], instead of the above formula, we can use the following formula:

$$B_{i,j}^{(l)} = \frac{1}{\eta_j-\eta_i}\frac{(\eta_j-\eta_0)\ldots(\eta_j-\eta_{i-1})(\eta_j-\eta_{i+1})\ldots(\eta_j-\eta_m)}{(\eta_i-\eta_0)\ldots(\eta_i-\eta_{i-1})(\eta_i-\eta_{i+1})\ldots(\eta_i-\eta_m)} \tag{3.6}$$

for $i \neq j$, and

$$B_{i,i}^{(l)} = \frac{1}{\eta_i-\eta_0} + \cdots + \frac{1}{\eta_i-\eta_{i-1}} + \frac{1}{\eta_i-\eta_{i+1}} + \cdots + \frac{1}{\eta_i-\eta_m} \tag{3.7}$$

for the diagonal components.

3.2 Total-discrete formulation

We consider $\mathbb{P}_m = span\{\psi_0, \psi_1, \ldots, \psi_m\}$ and defined the spectral element approximation space as

$$V_m^0 = \left\{ z \in H_0^1(I) : z|_\varepsilon \in \mathbb{P}_m(I) \right\}.$$

The Galerkin spectral element discretization problem can be described as:
Find $U^0, U^1, \ldots, U^n \in V_m^0$ such that

$$\frac{1}{k^2}\left(U^{n+1} - 2U^n + U^{n-1}, z\right) + \frac{\beta}{2k}\left(\frac{dU^{n+1}}{dx} - \frac{dU^{n-1}}{dx}, \frac{dz}{dx}\right) + \frac{\gamma}{3}\left(\frac{dU^{n+1}}{dx} + \frac{dU^n}{dx} + \frac{dU^{n-1}}{dx}, \frac{dz}{dx}\right) = \left(f^{n+1}, z\right). \tag{3.8}$$

The approximation solution U^{n+1} is estimated as

$$U^{n+1}(x) = \sum_{s=1}^{N_g} U^{n+1}(x_s)\psi_s, \tag{3.9}$$

where $N_g = N_e\,(m+1) - N_I$. The number of overlapping points of elements is set by N_I. By substituting (3.9) into (3.8), and taking $z = \psi_s$, yields the system:

$$\left[\mathcal{A}^g + \left(\frac{\beta k}{2} + \frac{\gamma k^2}{3}\right)\mathcal{B}^g\right]\mathcal{U}^{n+1} = \left[-\mathcal{A}^g + \left(\frac{\beta k}{2} - \frac{\gamma k^2}{3}\right)\mathcal{B}^g\right]\mathcal{U}^{n-1} + \left[2\mathcal{A}^g - \frac{\gamma k^2}{3}\mathcal{B}^g\right]\mathcal{U}^n + k^2\mathcal{A}^g F^{n+1}, \tag{3.10}$$

where $\mathcal{A}^g$ and $\mathcal{B}^g$ are the global matrices.

3.3 A priori error estimate

Definition 3.1. *[3] The projection operator $\Pi_h : H_0^1 \longrightarrow V_m^0$, is defined as*

$$\left(\frac{d}{dx}\left(u - \Pi_h u\right), \frac{dv}{dx}\right) = 0, \quad u \in H_0^1(I), \quad \forall v \in V_m^0. \tag{3.11}$$

Lemma 3.2. *[3] If $u \in H^s (s \geq 1)$, then*

$$\|u - \Pi_h u\| \leq C\left(\sum_{l=1}^{Ne} h^{2(\min(m+1,s)-1)} m^{2(1-s)} \|u\|_s^2\right)^{1/2}. \tag{3.12}$$

Definition 3.3. *We define the following two notations*

$$\Phi^{n+1} = u^{n+1} - \Pi_h u^{n+1}, \qquad \Upsilon^{n+1} = \Pi_h u^{n+1} - U^{n+1}.$$

Lemma 3.4. *[5] Assume that $\varepsilon^{n+1} = \Phi^{n+1} - \Phi^n$. Then there is a constant C such that:*

$$\|\varepsilon^{n+1}\| \leq C m^{(1-s)}. \tag{3.13}$$

Theorem 3.5. *Let $u(t_n)$ and U^n are the exact and approximate solution of* (2.4) *and* (2.8)*, respectively. Then, the subsequent error estimation is valid*

Proof. First, we consider the corresponding variational forms of (2.4) and (2.8), respectively, as follows:

$$\frac{1}{k^2}\left(u^{n+1}-2u^n+u^{n-1},z\right)+\frac{\beta}{2k}\left(\frac{du^{n+1}}{dx}-\frac{du^{n-1}}{dx},\frac{dz}{dx}\right)+\frac{\gamma}{3}\left(\frac{du^{n+1}}{dx}+\frac{du^n}{dx}+\frac{du^{n-1}}{dx},\frac{dz}{dx}\right)=\left(f^{n+1},z\right)+\left(R^t,z\right) \tag{3.14}$$

and

$$\frac{1}{k^2}\left(U^{n+1}-2U^n+U^{n-1},z\right)+\frac{\beta}{2k}\left(\frac{dU^{n+1}}{dx}-\frac{dU^{n-1}}{dx},\frac{dz}{dx}\right)+\frac{\gamma}{3}\left(\frac{dU^{n+1}}{dx}+\frac{dU^n}{dx}+\frac{dU^{n-1}}{dx},\frac{dz}{dx}\right)=\left(f^{n+1},z\right). \tag{3.15}$$

By subtracting (3.15) from (3.14), and adding and subtracting the projection operator (3.11), we derived

$$\begin{aligned}&\frac{1}{k^2}\left(\left(\Phi^{n+1}+\Upsilon^{n+1}\right)-2\left(\Phi^n+\Upsilon^n\right)+\left(\Phi^{n-1}+\Upsilon^{n-1}\right),z\right)\\&+\frac{\beta}{2k}\left(\frac{d}{dx}\left(\Phi^{n+1}+\Upsilon^{n+1}\right)-\frac{d}{dx}\left(\Phi^{n-1}+\Upsilon^{n-1}\right),\frac{dz}{dx}\right)\\&+\frac{\gamma}{3}\left(\frac{d}{dx}\left(\Phi^{n+1}+\Upsilon^{n+1}\right)+\frac{d}{dx}\left(\Phi^n+\Upsilon^n\right)+\frac{d}{dx}\left(\Phi^{n-1}+\Upsilon^{n-1}\right),\frac{dz}{dx}\right)\\&=\left(R^t,z\right)\end{aligned} \tag{3.16}$$

Base on the Definition 3.1, we have

$$\frac{1}{k^2}\left(\Upsilon^{n+1}-2\Upsilon^n+\Upsilon^{n-1},z\right)+\frac{\beta}{2k}\left(\frac{d\Upsilon^{n+1}}{dx}-\frac{d\Upsilon^{n-1}}{dx},\frac{dz}{dx}\right)+\frac{\gamma}{3}\left(\frac{d\Upsilon^{n+1}}{dx}+\frac{d\Upsilon^n}{dx}+\frac{d\Upsilon^{n_1}}{dx},\frac{dz}{dx}\right)=-\frac{1}{k^2}\left(\Phi^{n+1}-2\Phi^n+\Phi^{n-1},z\right)+\left(R^t,z\right). \tag{3.17}$$

Taking $z=\Upsilon^{n+1}-\Upsilon^{n-1}$ yields

$$\begin{aligned}&\left(\Upsilon^{n+1}-2\Upsilon^n+\Upsilon^{n-1},\Upsilon^{n+1}-\Upsilon^{n-1}\right)+\frac{\beta k}{2}\left(\frac{d}{dx}\left(\Upsilon^{n+1}-\Upsilon^{n-1}\right),\frac{d}{dx}\left(\Upsilon^{n+1}-\Upsilon^{n-1}\right)\right)\\&+\frac{\gamma k^2}{3}\left(\frac{d}{dx}\left(\Upsilon^{n+1}+\Upsilon^{n_1}\right),\frac{d}{dx}\left(\Upsilon^{n+1}-\Upsilon^{n-1}\right)\right)+\frac{\gamma k^2}{3}\left(\frac{d}{dx}\Upsilon^n,\frac{d}{dx}\left(\Upsilon^{n+1}-\Upsilon^{n-1}\right)\right)\\&=-\left(\Phi^{n+1}-2\Phi^n+\Phi^{n-1},\Upsilon^{n+1}-\Upsilon^{n-1}\right)+k^2\left(R^t,\Upsilon^{n+1}-\Upsilon^{n-1}\right).\end{aligned} \tag{3.18}$$

We can write the terms of the left side as

$$\left(\Upsilon^{n+1}-2\Upsilon^n+\Upsilon^{n-1},\Upsilon^{n+1}-\Upsilon^{n-1}\right)=\|\Upsilon^{n+1}-\Upsilon^n\|^2-\|\Upsilon^{n+1}-\Upsilon^{n-1}\|^2, \tag{3.19}$$

$$\left(\frac{d}{dx}\left(\Upsilon^{n+1}-\Upsilon^{n-1}\right),\frac{d}{dx}\left(\Upsilon^{n+1}-\Upsilon^{n-1}\right)\right)=\left\|\frac{d}{dx}\left(\Upsilon^{n+1}-\Upsilon^{n-1}\right)\right\|^2, \tag{3.20}$$

$$\left(\frac{d}{dx}\left(\Upsilon^{n+1}+\Upsilon^{n_1}\right),\frac{d}{dx}\left(\Upsilon^{n+1}-\Upsilon^{n-1}\right)\right)=\left\|\frac{d}{dx}\Upsilon^{n+1}\right\|^2-\left\|\frac{d}{dx}\Upsilon^{n-1}\right\|^2, \tag{3.21}$$

and also, by taking $\mathcal{H}^n = \Phi^{n+1} - 2\Phi^n + \Phi^{n-1}$, we can write the right side of (3.18) as

$$\begin{aligned}
&-\left(\mathcal{H}^n, \Upsilon^{n+1} - \Upsilon^{n-1}\right) + k^2(R^t, \Upsilon^{n+1} - \Upsilon^{n-1}) \\
&\quad \leq k^2\left(\mathcal{H}^n, \Upsilon^{n+1} - \Upsilon^{n-1}\right) + k^2(R^t, \Upsilon^{n+1} - \Upsilon^{n-1}) \\
&\quad \leq \frac{k^3 C_{\mathcal{P}}}{\beta}\|R^t\|^2 + \frac{k^3 C_{\mathcal{P}}}{\beta}\|\mathcal{H}^n\|^2 + \frac{\beta k}{2C_{\mathcal{P}}}\|\Upsilon^{n+1} - \Upsilon^{n-1}\|^2 \\
&\quad \leq \frac{k^3 C_{\mathcal{P}}}{\beta}\|R^t\|^2 + \frac{k^3 C_{\mathcal{P}}}{\beta}\|\mathcal{H}^n\|^2 + \frac{\beta k}{2}\left\|\frac{d}{dx}\left(\Upsilon^{n+1} - \Upsilon^{n-1}\right)\right\|^2. \qquad (3.22)
\end{aligned}$$

By subtracting (3.19)–(3.21) in (3.18), and the bound of (3.22) for the right side of (3.18), leads to

$$\begin{aligned}
&\|\Upsilon^{n+1} - \Upsilon^n\|^2 - \|\Upsilon^{n+1} - \Upsilon^{n-1}\|^2 + \frac{\beta k}{2}\left\|\frac{d}{dx}\left(\Upsilon^{n+1} - \Upsilon^{n-1}\right)\right\|^2 \\
&+ \frac{\gamma k^2}{3}\left\|\frac{d\Upsilon^{n+1}}{dx}\right\|^2 - \left\|\frac{d\Upsilon^{n-1}}{dx}\right\|^2 + \frac{\gamma k^2}{3}\left(\frac{d\Upsilon^n}{dx}, \frac{d}{dx}\left(\Upsilon^{n+1} - \Upsilon^{n-1}\right)\right) \\
&\leq \frac{k^3 C_{\mathcal{P}}}{\beta}\|R^t\|^2 + \frac{k^3 C_{\mathcal{P}}}{\beta}\|\mathcal{H}^n\|^2 + \frac{\beta k}{2}\left\|\frac{d}{dx}\left(\Upsilon^{n+1} - \Upsilon^{n-1}\right)\right\|^2. \qquad (3.23)
\end{aligned}$$

Summing the inequality (3.23) from 1 to n on time levels, conclude that

$$\begin{aligned}
&\sum_{j=1}^{n}\left(\|\Upsilon^{j+1} - \Upsilon^j\|^2 - \|\Upsilon^{j+1} - \Upsilon^{j-1}\|^2\right) + \frac{\gamma k^2}{3}\sum_{j=1}^{n}\left(\left\|\frac{d\Upsilon^{j+1}}{dx}\right\|^2 - \left\|\frac{d\Upsilon^{j-1}}{dx}\right\|^2\right) \\
&\quad + \frac{\gamma k^2}{3}\sum_{j=1}^{n}\left(\frac{d\Upsilon^j}{dx}, \frac{d}{dx}\left(\Upsilon^{j+1} - \Upsilon^{j-1}\right)\right) \leq \frac{k^3 C_{\mathcal{P}}}{\beta}\sum_{j=1}^{n}\|R^t\|^2 + \frac{k^3 C_{\mathcal{P}}}{\beta}\sum_{j=1}^{n}\|\mathcal{H}^j\|^2. \qquad (3.24)
\end{aligned}$$

Then, we have

$$\begin{aligned}
&\left(\|\Upsilon^{n+1} - \Upsilon^n\|^2 - \|\Upsilon^1 - \Upsilon^0\|^2\right) + \frac{\gamma k^2}{3}\left(\left\|\frac{d\Upsilon^{n+1}}{dx}\right\|^2 + \left\|\frac{d\Upsilon^n}{dx}\right\|^2 - \left[\left\|\frac{d\Upsilon^1}{dx}\right\|^2 + \left\|\frac{d\Upsilon^0}{dx}\right\|^2\right]\right) \\
&\quad + \frac{\gamma k^2}{3}\sum_{j=1}^{n}\left(\frac{d\Upsilon^j}{dx}, \frac{d}{dx}\left(\Upsilon^{j+1} - \Upsilon^{j-1}\right)\right) \leq \frac{k^3 C_{\mathcal{P}}}{\beta}\sum_{j=1}^{n}\|R^t\|^2 + \frac{k^3 C_{\mathcal{P}}}{\beta}\sum_{j=1}^{n}\|\mathcal{H}^j\|^2. \qquad (3.25)
\end{aligned}$$

We consider $\Upsilon^1 = \Upsilon^0 = 0$,

$$\frac{\gamma k^2 C_{\mathcal{P}}}{3}\left\|\frac{d\Upsilon^{n+1}}{dx}\right\|^2 \leq \frac{k^3 C_{\mathcal{P}}^2}{\beta}\sum_{j=1}^{n}\|R^t\|^2 + \frac{k^3 C_{\mathcal{P}}^2}{\beta}\sum_{j=1}^{n}\|\mathcal{H}^j\|^2. \qquad (3.26)$$

Using Poincare inequality, we have

$$\|\Upsilon^{n+1}\| \leq C_{\mathcal{P}}\left\|\frac{d\Upsilon^{n+1}}{dx}\right\| \leq Ck\sum_{j=1}^{n}\|R^t\| + Ck\sum_{j=1}^{n}\|\mathcal{H}^j\|. \qquad (3.27)$$

By the fact $\|R^t\| \leq \mathcal{O}\left(k^2\right)$ and using the triangle inequality and Lemma 3.2 for $\|\mathcal{H}^j\|$ as

$$\begin{aligned}
\|\mathcal{H}^j\| &= \|\left(\Phi^{n+1} - \Phi^n\right) - \left(\Phi^n - \Phi^{n-1}\right)\| \\
&\leq \|\varepsilon^{n+1}\| + \|\varepsilon^n\| \\
&\leq 2\max_{1\leq i\leq n}\|\varepsilon^{n+1}\| \\
&\leq \mathcal{O}\left(m^{(1-s)}\right),
\end{aligned}$$

Then,

$$\|\Upsilon^{n+1}\| \leq C_{\mathcal{P}} \left\| \frac{d\Upsilon^{n+1}}{dx} \right\| \leq C\left(T, C_{\mathcal{P}}\right)\left(k^2 + m^{(1-s)}\right). \tag{3.28}$$

Finally, by the triangle inequality, Lemma 3.4 and the inequality (3.28), we get

$$\begin{aligned} \|u^n - U^n\| &\leq \|\Phi^n + \Upsilon^n\| \\ &\leq Cm^{(1-s)} + C(T, C_{\mathcal{P}})\left(k^2 + m^{(1-s)}\right) \\ &\leq C^*\left(k^2 + m^{(1-s)}\right), \end{aligned} \tag{3.29}$$

this completes the proof. □

4 Numerical examples

This section provides an example for solution of the one-dimensional viscœlastic wave equation. The following relation will be used to verify the computational order:

$$\text{Order} = \log\left(e_1/e_2\right) / \log\left(k_1/k_2\right).$$

The numerical test is performed using MATLAB on a computer equipped with an Intel Core i5 processor and 6.00 GB of RAM

Example 4.1. *We consider the one-dimensional time viscœlastic wave equation with $\beta = 1$, $\gamma = 1$. The analytic solution is*

$$u(x,t) = \sin(2\pi x)e^{-t}. \tag{4.1}$$

Figure 1 displays the approximate solution solved using GLL-GSEM for $N_e = 10$, $m = 5$, and $k = 10^{-5}$ at $T = 1$, on the domain $I = [-1, 1]$ (left) and demonstrating high accuracy in absolute error (right). Table 1 reports the error in L_∞ for $N_e = 10$, and $m = 5$ at $T = 1$, on the domain $I = [0, 1]$. The numerical results clearly show that the convergence order in time is $\mathcal{O}\left(k^2\right)$, which aligns well with the theoretical analysis. Figure 2 illustrates that by decreasing the spatial step size for $m = 4$ (left) with $k = (N_e^4)$ at the final time $T = 1$, the resulting error decreases. We expect to observe an increase in round-off error with the increase in the number of elements. Additionally, we observe an increase in CPU time (Figure 2 right) with the increase in the number of elements. For the few the number of elements, we achieve high accuracy and acceptable CPU time by varying the interpolation degree, which is one of the advantages of the presented method.

Table 1: L_∞ error and order time for example 4.1.

k	L_∞	Order	CPU time
$1/4$	1.2018×10^{-2}	–	0.7155
$1/8$	2.9160×10^{-3}	2.04	1.0394
$1/16$	8.0691×10^{-4}	1.85	1.9019
$1/32$	2.0894×10^{-4}	1.94	3.5133
$1/64$	4.8175×10^{-5}	2.11	6.7965

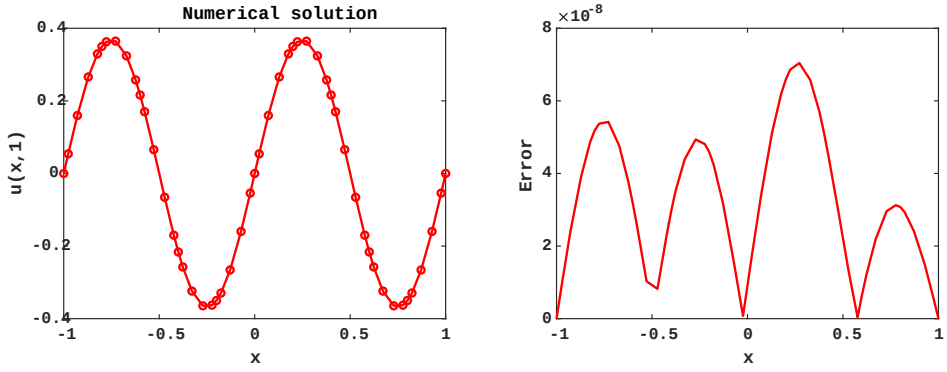

Figure 1: Left figure show the numerical solution and right figure show the L_∞ error (example 4.1).

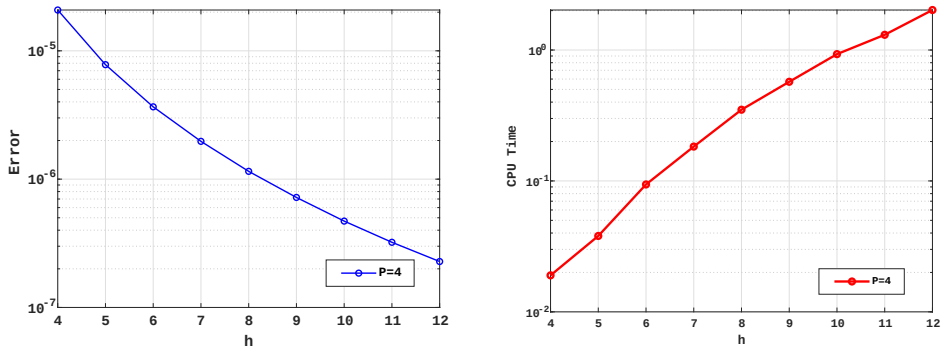

Figure 2: Left figure show the L_∞ error and right figure show CPU time (example 4.1).

5 Conclusion

In this study, we investigated the solution of the one-dimensional viscœlastic wave propagation model over time using the Galerkin Spectral Element Method (GSEM). We derived the semi-discrete formulation by applying second-order finite difference operators, and established second-order convergence in time. Subsequently, we implemented the GSEM using Gauss-Lobatto-Legendre (GLL) nodes. We also performed error analysis across successive time levels. Finally, the effectiveness of the proposed method was assessed through an example, demonstrating both its efficiency and high accuracy,with a time convergence order that aligns with the provided theoretical predictions. According to the error analysis and spectral convergence order of the presented method. This method can be used for two and dimensional viscœlastic wave equations in future. Its high accuracy makes it possible to obtain numerical solutions forviscœlastic wave equations in industry and physics.

References

[1] Aldirany, Z., Cottereau, R., Laforest, M., Prudhomme, S. (2022). Optimal error analysis of the spectral element method for the 2D homogeneous wave equation. Comput. Math. Appl., 119, 241-256.

[2] Belgacem, F., Bernardi, C. (1999). Spectral element discretization of the Maxwell equations. Math. Comput., 68(228), 1497-1520.

[3] Canuto, C., Hussaini, M.Y., Quarteroni, A., Zang, T.A. (2007). Spectral Methods: Evolution to Complex Geometries and Applications to Fluid Dynamics. Springer, Science & Business Media.

[4] Dehghan, M., Sabouri, M. (2012). A spectral element method for solving the Pennes bioheat transfer equation by using triangular and quadrilateral elements. Appl. Math. Model., 36(12), 6031-6049.

[5] Dehghan, M., Shafieeabyaneh, N., Abbaszadeh, M. (2020). Application of spectral element method for solving Sobolev equations with error estimation. Appl. Numer. Math., 158, 439-462.

[6] Dehghan, M., Shafieeabyaneh, N., Abbaszadeh, M. (2021). Numerical and theoretical discussions for solving nonlinear generalized Benjamin–Bona–Mahony–Burgers equation based on the Legendre spectral element method. Numer. Methods Partial Differ. Equ., 37(1), 360-382.

[7] Epperson, J. F. (1987). On the Runge example. Am. Math. Mon., 94(4), 329-341.

[8] Ern, A., Guermond, J.-L. (2004). Theory and Practice of Finite Elements. Volume 159. Springer, New York.

[9] Gharti, H.N., Oye, V., Komatitsch, D., Tromp, J. (2012). Simulation of multistage excavation based on a 3D spectral-element method. Comput. Struct., 100, 54-69.

[10] Jin, S., Luo, Z. (2019). A Crank–Nicolson collocation spectral method for the two-dimensional viscœlastic wave equation. Numer. Methods Partial Differ. Equ., 35(3), 1080-1092.

[11] Komatitsch, D., Erlebacher, G., Göddeke, D., Michéa, D. (2010). High-order finite-element seismic wave propagation modeling with MPI on a large GPU cluster. J. Comput. Phys., 229(20), 7692-7714.

[12] Komatitsch, D., Michéa, D., Erlebacher, G. (2009). Porting a high-order finite-element earthquake modeling application to NVIDIA graphics cards using CUDA. J. Parallel Distrib. Comput., 69(5), 451-460.

[13] Kronbichler, M.,& Persson, P.-O. (2021). Efficient High-Order Discretizations for Computational Fluid Dynamics. Cham, Switzerland: Springer International Publishing.

[14] Li M., & Nikan O., & Qiu W., & Xu D. (2022). An efficient localized meshless collocation method for the two-dimensional Burgers-type equation arising in fluid turbulent flows. Eng. Anal. Bound. Elem., 144, 44-54.

[15] Li, H., Zhao, Z., Luo, Z. (2016). A space-time continuous finite element method for 2D viscœlastic wave equation. Bound. Value Probl., 2016, 1-17.

[16] Luo, Z., Teng, F. (2017). An optimized SPDMFE extrapolation approach based on the POD technique for 2D viscœlastic wave equation. Bound. Value Probl., 2017, 1-20.

[17] Mehdizadeh, O.Z., Paraschivoiu, M. (2003). Investigation of a two-dimensional spectral element method for Helmholtz's equation. J. Comput. Phys., 189(1), 111-129.

[18] Nikan, O., Avazzadeh, Z. (2021). Coupling of the Crank–Nicolson scheme and localized meshless technique for viscœlastic wave model in fluid flow. J. Comput. Appl. Math., 398, 113695.

[19] Nikan, O., Avazzadeh, Z., Tenreiro Machado J.A. (2022). Numerical treatment of microscale heat transfer processes arising in thin films of metals. Int. J. Heat Mass Transf., 132, 105892.

[20] Oliveira, S.P., Leite, S.A. (2018). Error analysis of the spectral element method with Gauss–Lobatto–Legendre points for the acoustic wave equation in heterogeneous media. Appl. Numer. Math., 129, 39-57.

[21] Oruç, Ö. (2020). Two meshless methods based on local radial basis function and barycentric rational interpolation for solving 2D viscœlastic wave equation. Comput. Math. Appl., 79(12), 3272-3288.

[22] Patera, A.T. (1984). A spectral element method for fluid dynamics: laminar flow in a channel expansion. J. Comput. Phys., 54(3), 468-488.

[23] Pozrikidis, C. (2005). Finite and spectral element methods using Matlab. University of California San Diego, USA.

[24] Rong, Z., Xu, C. (2008). Numerical approximation of acoustic waves by spectral element methods. Applied Numerical Mathematics, 58(7), 999-1016.

[25] Sabouri, M., Dehghan, M. (2018). A hk mortar spectral element method for the p-Laplacian equation. Computers & Mathematics with Applications, 76(7), 1803-1826.

[26] Xia, H., Luo, Z. (2017). An optimized finite element extrapolating method for 2D viscœlastic wave equation. Journal of Inequalities and Applications, 2017(1), 1-18.

[27] Xia, H., Luo, Z. (2017). A POD-based–optimized finite difference CN-extrapolated implicit scheme for the 2D viscœlastic wave equation. Mathematical Methods in the Applied Sciences, 40(18), 6880-6890.

[28] Zampieri, E., Pavarino, L. F. (2006). An explicit second-order spectral element method for acoustic waves. Advances in Computational Mathematics, 25(4), 381-401.

[29] Zhao, Z., Li, H., Luo, Z. (2017). A space-time continuous Galerkin method with mesh modification for viscœlastic wave equations. Numerical Methods for Partial Differential Equations, 33(4), 1183-1207.